Severe Accident Analysis of a Station Blackout Accident Using MAAP-CANDU for the Point Lepreau Station Refurbishment Project Level 2 PSA

M.J. Brown and S.M. Petoukhov
(brownmj@aecl.ca)
Atomic Energy of Canada Limited, Chalk River Laboratories, Ontario, Canada

Abstract

A Level 2 Probabilistic Safety Assessment was performed for the Point Lepreau Generating Station, using the MAAP-CANDU code to simulate the progression of severe core damage accidents and fission product releases. Five representative severe accidents were selected: Station Blackout, Small Loss-of-Coolant, Stagnation Feeder Break, Steam Generator Tube Rupture, and Shutdown State. Analysis results for the reference station blackout accident are discussed in this paper.

1. Introduction

A Level 2 Probabilistic Safety Assessment (PSA) was performed by the Point Lepreau Refurbishment (PLR) Project of Atomic Energy of Canada Limited (AECL) for the Point Lepreau Generating Station (PLGS) CANDU® 6 reactor [1]. Reference [2] is an overview of PLGS operations and refurbishment. A Level 2 PSA quantified challenges to containment, and the location and species of fission product (FP) releases to the environment. Five representative severe core damage accidents were selected for the Level 2 PSA performed for the PLR Project:

1. Station blackout (SBO) accident;
2. Small loss-of-coolant accident (SLOCA);
3. Stagnation feeder break (SFB) LOCA [3];
4. Steam generator (i.e., boiler) tube rupture (SGTR) accident; and
5. Shutdown state accident (SSA) [4].

Each of these initiating accidents was analyzed for a reference case and several sub-cases with different availabilities of accident mitigation systems, e.g., emergency core cooling (ECC), steam generator (SG) feedwater. The reference SBO scenario (Case A) is discussed in this paper.

The MAAP-CANDU (Modular Accident Analysis Program for CANDU) code v4.0.5A+ [5] was used to estimate:

- The timing of the accident progression and accompanying thermo-physical and thermo-chemical phenomena,

® “CANDU” is a registered trademark of Atomic Energy of Canada Limited.

- The effect of safety system and normal operational system availabilities,
- Combustible gas sources, hydrogen and carbon monoxide concentrations in containment, and whether burning occurs (dependent upon oxygen and steam concentrations),
- FP transport and retention within reactor systems and containment,
- The timing, duration and magnitude of challenges to containment integrity,
- The size and nature of FP releases from containment to the environment, and
- The effect of operator actions in mitigating severe accident consequences (reducing challenges to containment integrity and reducing FP releases from the reactor building).

SBO reference Case A assumed no operator interventions and credited only a limited number of safety-related systems; the other systems were assumed unavailable. Twelve additional sensitivity cases were run, assuming various system availabilities to assess their effects on the accident sequence. Only results from reference Case A are discussed in this paper.

2. Brief Description of the MAAP-CANDU Code

MAAP-CANDU [5] can simulate severe accidents in CANDU stations, including many accident management actions. The code is based on the MAAP4 code developed by Fauske and Associates Inc. (FAI), owned by the Electric Power Research Institute, and used for severe accident analysis of light water reactors. Ontario Power Generation Inc (OPG) is the MAAP-CANDU code licensee, and AECL holds a sub-license from OPG.

3. Nodalization of the Point Lepreau Generating Station

MAAP-CANDU simulates the most significant systems and components necessary to demonstrate the overall response of the plant to a severe accident. The code tracks the mass and energy content of various heat sinks (liquid, solid and gas) within the Primary Heat Transport System (PHTS), calandria vessel (CV) and reactor building. It also tracks the location of FPs within the fuel, the PHTS, CV, containment, or released to the environment. Fluid momentum within the PHTS is not modelled, but some parameters can be adjusted so the PHTS response better emulates results from dedicated design basis thermalhydraulic codes. A primary purpose of MAAP-CANDU is the availability and use of heat sinks to absorb decay and chemical heat over an entire reactor building, for extended periods far beyond the life of the PHTS.

Some details of the MAAP-CANDU nodalization scheme, used to simulate the PLGS, are described here; additional details of the station nodalization were reported in Reference [1].

The containment is represented by 13 volumetric nodes, connected by 31 flow junctions. Concrete walls, floors and ceilings, and structural steel, are represented by 94 heat sinks. Adjacent rooms with large connecting openings are lumped together, as are similar heat sinks located in a node.

The PHTS is modelled for both loops, and each loop with two core passes. Seven nodes in each core pass represent the pump discharge line; reactor inlet header; reactor outlet header;

steam generator (SG) inlet piping; SG hot leg tubes; SG cold leg tubes; and the pump suction line connected to the SG cold leg. The 380 fuel channels are modelled with 36 characteristic fuel channels (2 loops × 6 vertical core nodes × 3 characteristic channels per vertical core node per loop). The 12 fuel bundles in each characteristic channel are modelled as 12 axial channel nodes. The fuel bundle, pressure tube (PT), and calandria tube (CT) of each axial channel node are modelled as nine concentric rings.

4. Model Operation / Component Failure Criteria

Key PLGS input parameters used in this study were presented in Table 1 of Reference [1]. A brief description of the model operation / component failure criteria is given in the following sections (see also References [1] and [5]). The assumptions were based on best estimates and engineering judgment, and do not reflect the only possible severe accident progression.

4.1 Containment failure

A simple failure junction models each of two airlocks (equipment and personnel) linking two different nodes in containment with the environment (service building, i.e., anything outside the containment boundary) [1]. A flow path forms between a containment node (containing an airlock) and the environment if the pressure difference exceeds 234 kPa; the inner and outer airlock door seals are assumed to fail simultaneously. The opening areas (0.0146 and 0.0039 m^2) represent the anticipated openings for airlock seal blowouts; the areas and pressure difference came from small-scale experiments of airlock seals. No other containment failure modes (e.g., containment cracking) are modelled because the required pressure is greater than 400 kPa (g).

4.2 Calandria vessel failure

MAAP-CANDU checks the CV conditions at every time step, to determine if any CV failure criteria has been met. In the current simulations, the CV is assumed to fail when the calandria vault water level decreases to the level of the top of the CV terminal debris bed, because that means there is insufficient external cooling in that region of the cylindrical CV shell. The CV is conservatively assumed to fail at the bottom, rapidly pouring all the terminal debris into the calandria vault (i.e., no debris is assumed to remain in the CV). Additional user-defined CV failure criteria (e.g., uncovery of the top of the vessel, pressurization due to PHTS rupture) could be coded in the input file, but were not considered in this study.

Due to the large surface area of the CV beneath the core debris, and the resulting relatively low heat flux, the water-filled calandria vault is assumed to be adequate for removing the corium heat. The insulating oxidic crust, the gap between the crust and the CV, and the adjacent heat sinks (water and steel ball-filled end shields, plus the water-cooled CV located above the core debris) reduce the CV temperature beneath the debris.

4.3 Fuel channel failure and fuel channel disassembly

Fuel channel failure is the perforation of its pressure boundaries followed by mass transfer between the inside of the PT and the CV (i.e., both the PT and CT fail). At high PHTS pressures, the channel is assumed to fail when a combined PT + CT creep (i.e., uniform ballooning) criterion is satisfied. The failed PHTS depressurizes into the CV, but no fuel channel debris is formed. A user could force a channel to fail earlier (e.g., to emulate local hot spots or steep PT thermal gradients), to determine the effect upon the overall severe accident progression, but only the built-in channel failure model was used in the current simulations.

At low PHTS pressures, fuel and channel material of an axial fuel channel node disassembles (i.e., separates from the remaining channel nodes to form debris) when the average PT and CT temperature reaches the oxygenated Zr melting point. The solid portion of the resulting debris is suspended, supported by underlying intact channels. If the underlying channels are immersed in the remaining moderator, they are assumed to be cool and strong enough to support the suspended debris until the core collapse criterion is met. As suspended debris continues to heat up, a molten component trickles down to the CV bottom. The suspended core debris is tracked by separate components until it moves to the CV terminal debris bed.

Channel sagging perforates the CT, allowing CV steam into the fuel channel annulus and increasing the channel heat up rate due to the exothermic Zr-steam reaction.

4.4 Core collapse

The suspended core debris is modelled to rapidly collapse to the bottom of the CV when the total suspended debris mass exceeds a user-specified value (25,000 kg per PHTS loop is used here, based on an assumption of the pull-out strength of cooled CTs).

4.5 Fission product release

MAAP-CANDU models the fuel elements as a mixture of UO_2 and the Zr fuel sheath. The fuel sheath is modelled to fail if the combined fuel sheath/UO_2 temperature of a radial channel node (i.e., fuel ring) reaches 1000 K (based on PHEBUS and BTF test results).

In the PLR analyses, inventories of only radioactive FPs were input to MAAP-CANDU. Fission products are modelled to be released from the fuel matrix based on fractional release models driven by the fuel temperature. The initial FP distribution is based upon the local heat generation at normal operating conditions. MAAP-CANDU does not model radioactive decay, but uses a total core decay heat curve. The decay heat is distributed amongst the FP groups based on a single time (the decay heat distribution does not change significantly past ~6 hours after reactor trip). MAAP-CANDU v4.0.5A+ assumes that no FPs are released from the terminal debris bed that accumulates on the bottom of the CV, because of the barrier provided by the top debris crust. Also, if the CV is dry when the terminal bed heats up enough to release FPs, there is no steam flow through the debris to transport FPs out of the CV.

5. Brief Description of the SBO Accident

This section describes the basic severe accident sequence anticipated for the SBO scenario. The processes or phenomena described in this section are modelled by MAAP-CANDU, some with greater sophistication than others. Several severe core damage processes (e.g., core debris formation and movement, debris - CV interaction) are complex, and are modelled based on engineering judgement due to a lack of experimental data. Some modelling assumptions are described (Section 6) as they can significantly affect the accident progression or consequences.

The SBO accident sequence starts with a loss of power, tripping the reactor and causing the loss of pumps (e.g., PHTS, moderator cooling, shield cooling, SG feedwater, and recirculating cooling water). The accident progresses to core damage because of the loss of: i) PHTS inventory, ii) long-term emergency core cooling (ECC), iii) moderator cooling, and iv) shield and calandria vault cooling. Some sensitivity cases credited safety-related functions (e.g., ECC, crash cool-down); these systems tended to delay the accident progression and change the FP releases, but did not halt the accident unless long-term cooling was maintained/restored (e.g., low pressure ECC with a heat exchanger, or calandria vault cooling).

The basic SBO accident sequence (no mitigating systems), as modelled by MAAP-CANDU:

a) Reactor initially at full power and pressure. At time = 0 s, station loses Class IV and Class III power, tripping reactor and pumps (end of active heat sinks).
b) Without feedwater, SG secondary side water boils off at main steam safety valve (MSSV) opening pressure, removing short term decay heat. PHTS temperature and pressure stay high.
c) SG dryout is loss of major heat sink. PHTS heats up and pressurizes until liquid relief valves (LRVs) open, venting primary coolant into degasser condenser (DC). DC pressurizes, vents to containment. Containment pressurization triggers dousing.
d) Loss of primary coolant (water, then steam) through LRVs uncovers fuel. Dry fuel channels overheat and rupture, depressurizing PHTS (remaining primary coolant discharges into CV).
e) Fuel channel rupture pressurizes CV, CV rupture disks burst. Some moderator expelled into containment via CV relief ducts. Remaining moderator boils off as fuel channels dry out on inside, increasing heat to moderator.
f) Dry fuel channel sections (uncovered on CT outside) overheat, disassemble and drop onto lower intact channels cooled by remaining moderator. Some debris relocates to CV bottom, quenched by remaining moderator.
g) Majority of core drops to bottom of CV (slowly or by core collapse). Remaining moderator boiled off by debris decay heat.
h) Calandria vault water cools outside of CV and thus core debris.
i) Calandria vault water boils off. CV assumed to fail by debris heat-up after vault water level decreases to elevation of top of debris in CV.
j) Core debris relocates onto calandria vault floor. Remaining vault water boiled off.

k) Debris heats up; molten core concrete interaction (MCCI), calandria vault floor melt through.
l) Molten corium relocates to reactor building basement, quenched by remaining water.

The airlock seals (containment) may fail during many of the events listed above, in particular during periods of rapid steam generation (*g*: core collapse, *i*: CV failure, *k*: calandria vault failure) that cause pressure peaks.

During many of the accident stages, hot core debris can release FPs from the fuel. The release rate can be significant during the suspension of hot core debris in the CV, and during MCCI.

The above accident sequence has many places where user-input and code assumptions significantly influence the accident sequence / timing. e.g., an earlier core collapse reduces the time that debris is suspended in the CV, thus reducing the hydrogen produced and FPs released in that stage of the accident. An earlier core collapse may also reduce the pressure peak caused by the debris being quenched, perhaps avoiding containment failure at that time.

6. SBO Analysis Assumptions

The SBO initiating event was the loss of Class IV and III power at time = 0 s. The simulations were run to 500,000 s (139 h); a mission time of 72 h was required for the Level 2 PSA.

The following assumptions applied to all the SBO-initiated severe accident simulations:

1) The total heat generation in the reactor, at time = 0 s, was 2,156 MW (th). This included the gamma heat deposited in the moderator.
2) Class IV and Class III electrical power supplies were lost at time = 0 s, and not recovered.
3) Reactor shutdown occurred at time = 0 s (reactor tripped on loss of Class IV).
4) Primary pumps ran down and the moderator cooling, shield cooling and shutdown cooling systems became unavailable at time = 0 s (no power for pumps). Local air coolers also unavailable due to loss of power.
5) Main SG feed water lost at time = 0 s. Auxiliary steam-driven SG feedwater unavailable.
6) PLGS SGs are linked by a common steam header, and there are no main steam isolation valves (MSIVs). Upon loss of Class IV, the turbine emergency stop valve would close, isolating the turbine from the SG common header. The loss of the condenser circulating water pumps would disable the condenser and prevent the condenser steam discharge valves from opening, so the SG pressure would rise. No MAAP-CANDU models of the secondary side downstream of the SGs were available for this analysis. However, the behaviour in each SG would be almost identical, following loss of power, so the MSIV model was used to separate the SGs from each other and from the turbine and condenser.
7) PHTS loop isolation was not credited because the isolation valves require power.
8) AECL passive autocatalytic recombiners (PARs) were credited. There were 19 PARs: 8 in containment Node 1 (basement), 1 in Node 2 (stairwell to SG room), 1 in Node 5

(portions of floors 1, 2, 3 and 4), 8 in Node 8 (lower SG room), and 1 in Node 9 (moderator service area).

9) The LRVs and pressurizer relief valves were modelled to discharge primary coolant directly to containment. In reality, these valves discharge into the degasser condenser (DC), which was not modelled in these analyses. This assumption is conservative, because the DC would have provided additional 20 m^3 volume to contain high pressure PHTS steam or liquid while the loops were intact, delaying and reducing coolant venting into containment and slowing containment pressurization. Some FPs could be deposited in the DC prior to loop rupture, although FP releases from the fuel were low until core disassembly.

10) Moderator cover gas system bleed valves, connecting CV and vapour recovery system, were assumed operable but failed open after 7,200 s (their air reservoirs were assumed depleted). These valves allowed some moderator (water or steam) to leave the CV.

11) The SG main steam safety valves (MSSVs) were available; they opened and closed at their set point (5.11 MPa) to relieve the SG secondary side pressure.

12) Containment isolation was assumed to be effective from time = 0 s. In reality, this system would operate if containment pressure increased to 3.5 kPa (g), due to the loss of local air coolers and any hot water or steam entering containment from the PHTS or CV. In the SBO simulations the containment pressure increased to 3.5 kPa (g) at time = ~200 s.

13) The primary coolant was initially modelled as a single-phase liquid in each PHTS loop, with no loop void. As the void fraction increased, due to the LRVs opening, coolant was modelled as a homogeneous two-phase fluid. When the loop void fraction exceeded 50% (a user input), the primary coolant in that loop separated into water and steam. The water was tracked in separate pools corresponding to PHTS nodes and fuel channels.

The above assumptions applied to all SBO simulations, but some assumptions were varied:

i. SG crash cool-down: available or unavailable (unavailable in reference case).

ii. High, medium and low pressure ECC injection stages: available or unavailable (unavailable in reference case). The LP ECC heat exchanger, for cooling the sump water before it was pumped into the PHTS, was also available or unavailable. All ECC functions and capabilities were unavailable in the reference Case A.

iii. Containment dousing: available or unavailable (unavailable in reference case) with a total capacity of 1.38x106 kg of water and maximum water flow rate of 2,145 kg/s.

iv. Emergency Power Supply (EPS): unavailable or available (unavailable in reference case), used to power the ECC recovery pump, which injected sump water into the PHTS.

v. Moderator drain: assumed or not (not assumed in reference case). A PT + CT rupture can also rupture the fuel channel bellows, causing the moderator to drain at 4.2 kg/s per ruptured channel. MAAP-CANDU models a maximum of one channel failure per PHTS loop, because it assumes one failed channel will depressurize the PHTS before another channel can rupture.

vi. Containment leakage was modelled (as in reference case) by an opening to environment that allowed 2.5% of containment volume to leak out per 24 hours, given a pressure difference of 124 kPa. One sensitivity case doubled the leakage rate.

7. Reference Case A Analysis Results

The results of key parameters are shown in Figures 1 to 14, and the key event times in Table 1.

7.1 Primary heat transport system and steam generator response

The Case A station blackout began at 0 s, which tripped the reactor and stopped the fission heat source. The SGs continued to remove large amounts of heat by boiling the secondary side water and venting the steam through the MSSVs, which maintained the SG pressure at 5.1 MPa (a) (Figure 1) until a fuel channel failed at 14,288 s (3.9 h). This cooled the PHTS coolant, so the loops depressurized to ~9 MPa(a) (Figure 2) until about 5,000 s (~1.4 h), when the SG secondary side water level (Figure 3) had decreased so that it could no longer provide adequate heat removal from the PHTS.

The pressurizer water flowed into the PHTS during the first ~200 s, as the PHTS water cooled and its density increased. The loop water masses increased from 44,474 kg (Loop 1) and 45,030 kg (Loop 2) to ~50,000 kg per loop (Figure 4). The PHTS and pressurizer water masses and levels then remained essentially constant until ~5,000 s (1.4 h). As the SGs dried out, the primary coolant temperature increased; the thermal swell pushed loop water back into the pressurizer, and the water mass in both loops decreased.

The last of the SG secondary side water boiled off in both loops at ~6,700 s (1.9 h), ending the heat sink for the PHTS (Figure 3). The PHTS kept the SGs hot, and the MSSVs set point kept the pressure at ~5.1 MPa; the SG pressure did not begin to decrease until a fuel channel failed at 14,288 s (3.9 h). After the channel rupture, the secondary side of the SGs depressurized slowly during the rest of the simulation, cooled by the containment atmosphere (Figure 1).

The PHTS pressure increased to 10.16 MPa (a) by 6,636 s (1.8 h, Figure 2). The LRVs began to open and close (Figure 5), discharging PHTS liquid to containment and preventing the PHTS pressure from rising further. The pressurizer water level continued to rise, but at a slower rate, because the LRV flow accommodated most of the primary coolant volume change.

The primary coolant in both loops reached saturation conditions (10.16 MPa, 312°C) at 7,697 s (2.1 h). The core heat was no longer absorbed by the sensible heat of water, but rather by the latent heat of boiling. Thus the coolant volume change per unit of input heat increased by a factor of ~18, so the LRVs had to discharge 18 times as much volume to keep the PHTS pressure constant. The modelled LRVs were unable to cope with the volume change rate, and thus stayed open continuously as the PHTS pressure increased to a maximum of 11.5 MPa(a) at 8,760 s (2.4 h, Figure 2).

At ~9,000 s (2.5 h), the average loop void fractions increased to 50% (Figure 5), the user-input value at which the PHTS fluid was assumed to separate into liquid and gas phases. The LRV flow changed from homogeneous two-phase flow to stratified two-phase flow, because the top of the collapsed liquid was at approximately the same height as the LRV opening. The LRV vapour flow rate increased from ~1 kg/s to 7.5 kg/s, and the liquid flow rate decreased from ~18 kg/s to 0 kg/s during the switchover period. This translated into a change in LRV volume flow rate (per PHTS loop) from ~0.04 m^3/s to ~0.14 m^3/s. This threefold increase in the LRV volume flow rate permitted the PHTS to depressurize to the LRV opening pressure by 9,801 s (~2.7 h). After that, the LRVs opened and closed to vent vapour, as necessary.

As the PHTS loop void fractions increased, the loop water masses decreased rapidly (Figure 4). The remaining pressurizer water entered the PHTS loops, until the pressurizer emptied at 8,802 s (2.4 h). After that, the loop inventory decreased more rapidly because there was nothing left to replace the expelled coolant. When LRV flow switched from two-phase fluid to steam at ~9,000 s (2.5 h), the primary coolant loss rate decreased and the primary water was being used to its full capacity for removing heat (i.e., no more water was being expelled, only steam).

As the loop water decreased, fuel began to be exposed in both loops at~9,900 s (2.7 h). In MAAP-CANDU, the fuel and fuel channel heat up is not modelled until the characteristic channel is predicted to be dry (i.e., less than 1 kg of water remaining in the fuel channel). All model fuel rings heat up once the channel is dry. MAAP-CANDU simulates the change in heat transfer to the primary coolant, as the water level decreases in the channels; the heat to the channel coolant decreases, while the heat to the moderator and end shields increases.

At 14,288 s (4.0 h), Loop 2 characteristic Channel 7 ruptured, due to high PHTS pressure (10.2 MPa (a)) coincident with high fuel channel temperatures. Both PHTS loops rapidly depressurized (Figure 2) to 0.2 MPa (a), because the loops were not isolated (isolation valves are power-operated). The PHTS water mass decreased to ~2,000 kg/loop (Figure 4), which marked the end of the PHTS portion of this accident simulation.

During an SBO accident, both PHTS loops would be at essentially the same pressure and water levels decrease at the same rate, because there is no loop isolation. Thus the same characteristic channels in each loop would have similar thermal and pressure conditions. Small perturbations in the code calculation process, or small physical differences (e.g., initial loop volumes), will likely cause one loop to approach fuel channel rupture more rapidly than the other loop. The resulting depressurization of both loops removes the driving force for the remaining intact loop to rupture. The PLGS simulations had slightly different loop volumes, so the PHTS behaviour was slightly different between the loops, and typically one loop sustained a channel failure while the other loop did not. In one sensitivity case, both loops sustained channel ruptures.

7.2 Fuel and fuel channel response

Fuel began to be exposed in both loops at~9,900 s (2.7 h). Characteristic Channel 1 was the first to dry out (less than 1 kg water in the channel) in each loop, at ~14,100 s (3.9 h). When a channel is deemed dry, channel heat up is calculated; the fuel, PT and CT temperatures start to increase due to the decay heat and, at higher temperatures, the Zr-steam reaction. Until channels are declared dry, the fuel, PT and CT temperatures are assumed to be constant at location-dependent user input values (Fuel: ~600 to 1200 K; PT: ~540 to 580 K; CT: 343 K).

At 14,288 s (4.0 h), Loop 2 characteristic Channel 7 ruptured due to high PHTS pressure concurrent with elevated PT temperatures. The break area corresponded to a guillotine break of one fuel channel. The ruptured channel discharged primary water and steam (and a small amount of hydrogen) into the CV. The Channel 7axial nodes stayed intact (i.e., did not form debris) after rupture, because the CT was still immersed in moderator and was thus cool and strong. Axial channel Node (i.e., bundle) 6, of Channel 1 in Loop 2, was the first to disassemble at 19,669 s (5.5 h), and the first Loop 1 channel node disassembled 12 s later.

Example fuel and fuel channel temperatures, of the 7th axial channel node (bundle) of Loop 1 characteristic Channel 1 (representing four high power channels in the topmost core node), are shown in Figure 6. The temperatures increased when the PT dried out at 14,084 s (3.9 h). Initially the CT heated up to about 420 K, indicating nucleate boiling on the outside. After the CV rupture disk burst, some moderator was expelled and the level decreased below the bottom of the channel (Figure 7). This removed the CT heat sink, so fuel and fuel channel temperatures increased further. The two-phase moderator level increased at ~15,500 s (due to boiling) and recovered the CT, cooling it to ~400 K. The CT remained cool until ~18,000 s (5 h), and the PT and fuel temperatures decreased. The moderator level decreased again due to boil off, and the CT was again uncovered; the fuel and fuel channel temperatures then increased until the fuel channel node disassembled to debris at 21,591 s (6.0 h). MAAP-CANDU sets fuel and fuel channel temperatures to 0 K to indicate a channel node has disassembled to debris.

7.3 Calandria vessel response

During the early stages of the accident progression, the moderator slowly heated up because of the loss of the moderator cooling system and the addition of decay heat from the fuel. Heat was transferred from the PHTS across the fuel channel annuli to the moderator, and was also directly deposited in the moderator by absorbing gamma radiation from the fuel. Figure 7 shows the level of the two-phase moderator mixture.

As the moderator heated, it swelled (thermal expansion) from the initial height of 8.05 m to 8.26 m by 1,603 s. At that time the pressure difference, between the CV and containment, first exceeded the user input differential of 29 kPa (g); this caused the moderator bleed valves to begin opening and closing to keep the pressure difference at 29 kPa (g). Opening the valves slowed the CV pressurization to match the rise rate in containment; it also released some moderator to containment, resulting in a small decrease in the moderator level.

The CV pressure (Figure 8) increased as the accident progressed and the moderator heated up, increasing the partial pressures of steam and the cover gas. The moderator bleed valve maintained a pressure difference of 29 kPa (g) between the CV and the containment. At 7,200 s, the air-operated CV bleed valves were assumed to fail open, because the air reservoir was assumed depleted, and so the CV depressurized to the containment pressure. As the moderator heated further, the water swelled due to thermal expansion and covered the junction to the bleed valve; this reduced the volume flow rate through the bleed valve and the CV pressure could no longer be completely relieved. Thus the CV pressure increased above the containment pressure, for time beyond ~11,000 s (3 h).

At 14,288 s (4.0 h), Loop 2 characteristic Channel 7 ruptured, adding hot pressurized PHTS steam to the moderator, which increased the moderator mixture level (Figure 7). The moderator soon began to boil, due to the decay and gamma heat plus the hot steam from the PHTS. The pressurization burst a CV relief duct rupture disk at 14,531 s (4.0 h). The sudden CV pressure drop caused flash boiling and a rapid expulsion of water out the open relief duct. Approximately 69,000 kg of water was expelled in ~440 s following the CV rupture disk bursting.

By 15,000 s, only ~155,000 kg (67%) of the initial 229,810 kg of moderator was left in the CV. Most of the lost moderator was expelled from the CV as water, thus reducing the moderator heat sink without the benefit of undergoing a phase change. Following the CV rupture disk bursting, the CV pressure remained about 30 kPa higher than containment, due to the pressure drop in the flow of steam discharging from the CV. When the moderator finished boiling off at 39,005 s (11 h), the pressure drop decreased because there was no longer any significant discharge; the CV pressure matched that of containment for the remainder of the simulation (Figure 8).

Fuel channel disassembly began at 19,681 s (5.5 hin Loop 1, and 19,669 s in Loop 2. The mass of UO_2 remaining in the intact core (Figure 9) decreased in steps; small steps represent a few axial channel nodes (including all corresponding nodes in the associated channels), and larger steps represent several individual nodes or a string of nodes from one or more characteristic channel. The total mass of suspended debris increased as channels disassembled, while some suspended material (molten and solid) moved to the CV terminal debris bed, where it was quenched in the remaining moderator. The mass of suspended debris never reached the 25,000 kg/loop core collapse criterion in either loop, so the core disassembled and relocated to the CV terminal bed in a relatively smooth fashion.

About 12% of the Loop 1 channel nodes, and 10% of the Loop 2 channel nodes, remained intact after the main core disassembly finished at ~39,000 s (11 h, Figure 9). Another ~9% of the remaining intact fuel channel nodes disassembled between 43 and 44 h, and the last ~3% disassembled between 48 and 101 h. The last ~11% of the core to disassemble consisted mainly of the stub ends of low power channels (i.e., those around the periphery of the CV).

The CV terminal debris began to heat up after the moderator had boiled off. Some heat was transferred from the debris bed by conduction through the lower CV wall (which was immersed in the calandria vault water) and by radiation from the top surface to the upper CV walls (also immersed in calandria vault water). The solid particulate material began to melt soon after the last of the moderator boiled off (Figure 10). At ~55,000 s (15 h), the last of the particulate debris had melted to form the molten debris pool, or had re-solidified into a bottom crust (~5 to 10 cm thick) in contact with the lower CV wall and a top crust cooled by radiation to the CV walls.

The calandria vault water level decreased to the level of the top of the CV debris bed at 166,187 s (46 h), so the CV wall was assumed to fail at the bottom of the vessel. All the core debris then relocated out of the CV and onto the calandria vault floor; no crust was assumed to remain in the CV. An energetic interaction between the corium and calandria vault water was predicted.

7.4 Calandria vault and end shields response

The pressure (Figure 8) and water level (Figure 11) in the calandria vault and end-shields increased gradually after time = 0 s, due to the unavailability of the shield and moderator cooling systems and the resulting thermal expansion of the calandria vault water. The calandria vault and end-shields are connected via combined vent lines, which can relieve over-pressure via rupture disks. At 15,580 s (4.3 h), these rupture disks burst due to the steam generated in the end shields. Steam discharged to containment, and the end-shield water level decreased. The calandria vault water began to boil at 49,854 s (13.8 h), resulting in a gradual decrease of the water level.

The CV failed at 166,187 s (46 h), and all the core debris poured onto the calandria vault floor (Figure 10). The calandria vault water boiled off faster than previously due to the water contacting a larger surface area of core debris; by 190,530 s (53 h) the last of the water boiled off.

The corium temperature then increased due to the decay heat, and MCCI began at 200,371 s (56 h). When the concrete floor eroded to a depth of 2 m at 431,600 s (120 h), the calandria vault was assumed failed. The debris relocated to the reactor building basement where it was quenched in water, resulting in a final containment pressure spike (Figure 8).

7.5 Containment response

Figure 8 shows the pressure in the lower half of the SG enclosure, which was open to the rest of containment. Initially, the pressure was about 101 kPa (a). The containment pressure increased because of the following processes: hot PHTS coolant discharged through the PHTS LRVs beginning at 6,636 s (1.8 h); the CV rupture disk burst at 14,531 s (4.0 h), following the rupture of Loop 2 Channel 7 and the moderator boiling at 14,494 s (4.0 h); the calandria vault rupture disk burst, venting to containment, at 15,580 s (4.3 h); and the core disassembled and relocated, which boiled off the remaining moderator. All of these processes increased the containment pressure until both airlock seals blew out at 29,200 s (8.1 h).

The containment pressure then decreased almost to atmospheric pressure. At 49,854 s (13.8 h), the calandria vault water reached saturation conditions. The increased steam flow into containment exceeded the sum of the efflux through the blown out airlock seals and the condensation within containment, so the containment pressure slowly began to increase again (Figure 8). It reached a maximum of 139 kPa (a) at 106,956 s (30 h), after which the discharge plus condensation exceeded the steam generation.

The pressure declined slowly to 112 kPa(a), just prior to the failure of the CV at 166,187 s (46 h), when corium relocated into the calandria vault. The corium quenched, in the remaining calandria vault water, generating a large amount of steam and caused a sharp rise in containment pressure to a peak of 271 kPa(a).

The calandria vault water was boiled off by 190,530 s (53 h), so the steam generation stopped and the containment pressure decreased to atmospheric pressure by 200,000 s (56 h). The MCCI began in the calandria vault at 200,371 s (56 h), but the gas generation from the MCCI was lower than the flow rate through the blown out airlock seals. Therefore, the containment remained depressurized (Figure 8).

The rapid increase in the containment pressure at 431,600 s (120 h) was due to corium relocating into the basement after the calandria vault failure and subsequent corium quenching. The containment pressure decreased after reaching a peak pressure of 534 kPa (a), because of condensation on the containment walls and internal structures, plus the discharge through the failed airlock seals. The simulations for this report did not employ a criterion for a global failure of the reactor building, only the possibility that the airlock seals could blow out. Containment pressure decreased to 159 kPa (a) by the end of the simulation at 500,000 s.

7.6 Fission product release and distribution

Initially, there was 1.04 kg of noble gas (Kr + Xe, radioactive isotopes only) in the core. After the first fuel element temperatures exceeded 1000 K (14,104 s, 3.9 h), FPs began to be released from fuel elements. Most of the noble gas inventory was released into the CV from the fuel and suspended debris bed during core disassembly (Figure 12, ~5.5 h to ~11 h), when temperatures were high. The noble gas escaped to containment through the burst CV rupture disks. Some then escaped to the environment via containment leakage and through the blown out airlock seals (after 8.1 h). About 95% of the noble gas was released to the environment, by 30 h.

Figure 13 shows the mass of radioactive iodides released from fuel and debris inside the CV, and from the containment to the environment. The initial inventory of Cs, I and Rb in the core (radioactive isotopes) was 17.1 kg. Fission products were released to the CV from the PHTS and from the suspended debris bed. FPs were transported into containment after the CV rupture disks burst at ~4 h. It was assumed that the corium crust, formed in the CV, prevented significant FP releases. When the CV failed, the crust failed but the debris was quenched in the remaining calandria vault water, so any further FP releases would have been very low. A small additional amount of the iodides was released later from suspended debris in the CV, but little was released from the ex-vessel MCCI. No FP releases were modelled to occur in the calandria vault until the MCCI began.

At the end of the simulation (500,000 s), the total mass Cs, I and Rb (radioactive isotopes) released to the environment (in iodide and hydroxide forms) was 1.25 kg or 7.3% of the initial inventory of these isotopes.

7.7 Hydrogen release

Hydrogen was released by steam reacting with Zr in hot and dry fuel channels, and in the suspended debris beds of both PHTS loops. It also occurred due to MCCI. The first fuel channels dried out in both loops at ~6,700 s (~1.9 h). Steam inside dry channels reacts with Zr fuel cladding and the inner surface of the Zr pressure tube, producing hydrogen, and the reaction rate increases with temperature (Figure 14). The hydrogen production increased after core disassembly started at ~5.5 h (both loops). At ~10.8 h the CV was dry, so hydrogen production significantly decreased without fresh steam. A small amount of hydrogen was produced from the few remaining intact channel stubs in the CV. The solid crust, formed on the top of the CV terminal debris bed, was assumed to prevent steam access and FP release.

A total of 304 kg of hydrogen was produced, during the core heat up and disassembly, inside the PHTS loops and from the debris suspended inside the CV. This corresponds to ~17.6% of the initial in-core Zr inventory being consumed. An additional 72 kg of hydrogen was produced in the CV, and a further 2,452 kg of hydrogen was produced in the calandria vault due to MCCI.

No hydrogen or carbon monoxide burning in containment was predicted in Case A, due to the airlock seals failure and the subsequent steam generation purging containment.

7.8 Sensitivity cases

As mentioned, a total of thirteen SBO cases (including reference Case A) were analyzed for the PSA Level 2 activities for PLGS Refurbishment Project. Sensitivity cases credited various plant safety-related features/operator actions, but the results are beyond the scope of this paper.

8. Summary

A series of thirteen simulations were run to assess the consequences of a severe accident, beginning with a station blackout, in the Point Lepreau CANDU 6 generating station. This was done for a Level 2 probabilistic safety assessment, for the PLGS refurbishment. The accident began with a loss of Class III and Class IV power, while the reactor was at full power. The simulations were run with the severe accident analysis code MAAP-CANDU v4.0.5A+, using the PLGS specific parameter file.

This paper discusses major results of SBO reference Case A, which assumed most safety-related plant systems were not available:

Unavailable: Class III and Class IV power, main and auxiliary SG feedwater (main and auxiliary), emergency water supply, loop isolation, moderator cooling, shield cooling, shutdown cooling, and emergency core cooling (all stages);

Available: Reactor shutdown, dousing spray, containment isolation, AECL PARs, SG main steam safety valves.

In reference Case A, severe core damage began at 5.5 hours, the moderator finished boiling off in the CV at 10.8 h, containment failed at 8.1 h, and the CV failed at 46 h. The total release of radioactive isotopes of Cs, Rb and I was 7.3% of their initial inventory. Almost the entire initial noble gas core inventory was carried by the containment atmosphere to the environment, primarily after containment failure. No hydrogen/carbon monoxide burning was predicted.

9. Acknowledgements

The authors wish to thank the following individuals for their contribution to the paper:

Chan Y. Paik (FAI), Liliana Comanescu (Candu Energy), Mark Yandt and Barbara Pruszkowski (AECL); Ghulam Khawaja (OPG), and all reviewers.

10. References

[1] S.M. Petoukhov, M.J. Brown and P.M. Mathew, "MAAP4-CANDU Application to the PSA Level 2 for the Point Lepreau Nuclear Generating Station Refurbishment Project", 30th Annual Canadian Nuclear Society Conference, Calgary, Alberta, 2009 June.

[2] R. Eagles, "Point Lepreau Generating Station Refurbishment Project - Update and Status", 28th Annual Conference of the Canadian Nuclear Society, Saint John, New Brunswick, 2007 June.

[3] S.M. Petoukhov and G.M. Khawaja, "Severe Accident Analysis Of Stagnation Feeder Break Scenarios Using MAAP4-CANDU For Application To The Level 2 PSA For The Point Lepreau Station Refurbishment Project", 32nd Annual Conference of the Canadian Nuclear Society, Niagara Falls, Ontario, 2011 June.

[4] S.M. Petoukhov, M.J. Brown and P.M. Mathew, "Severe Accident Analysis Of Shutdown State Accident Using MAAP4-CANDU To Support Level 2 PSA For The Point Lepreau Station Refurbishment Project", 32nd Annual Conference of the Canadian Nuclear Society, Niagara Falls, Ontario, 2011 June.

[5] P.M. Mathew, S.M. Petoukhov and M.J. Brown, "An Overview of MAAP4-CANDU Code", 28th Annual Conference of the Canadian Nuclear Society, Saint John, New Brunswick, 2007 June.

Table 1
Sequence of significant events for station blackout scenario, reference Case A

Time (hr)	Time (s)	Event
0.0	0	AC power loss (Class IV & III) causes reactor trip
0.0	0	Turbine stop valves closed (MAAP-CANDU does not model them)
0.0	0	Primary pumps off, moderator cooling and circulation off, shield cooling system off, SG main and auxiliary feed water pumps off
0.4	1,603	Calandria vessel bleed valve opens
1.8	6,636	LRVs open for the first time, PHTS Loops 1 & 2
1.9	6,688	SG secondary sides are dry, Loop 2
1.9	6,693	SG secondary sides are dry, Loop 1
2.0	7,178	Dousing system starts
2.2	7,840	Dousing system exhausted (dousing max flow rate 2142 kg/s)
2.4	8,802	Pressurizer empty
3.9	14,084	At least one channel is dry Loop 2 (complete boil-off) – Channel 1
4.0	14,248	At least one channel is dry Loop 1 (complete boil-off) – Channel 1
4.0	14,288	PT & CT ruptures in Loop 2 – Channel 7
4.0	14,494	Moderator reaches saturation temperature
4.0	14,531	Calandria vessel rupture disk open, connecting to SG room
4.3	15,580	Calandria vault rupture disk open, connecting to SG room
5.5	19,669	Beginning of the core disassembly, Loop 2
5.5	19,681	Beginning of the core disassembly, Loop 1
N/A	N/A	Loop 1 core collapse to CV bottom (does not occur in Case A)
N/A	N/A	Loop 2 core collapse to CV bottom (does not occur in Case A)
8.1 8.1	29,207 29,242	Large airlock seals failed (Junction 30) = Containment failed Small airlock seals failed (Junction 31)
11	39,005	Water depleted inside calandria vessel
14	49,854	Water in calandria vault reaches saturation temperature
46	166,187	Calandria vessel failed
46	166,188	Energetic core-debris steam interaction occurred in calandria vault
53	190,530	Water depleted inside calandria vault (Node 10)
56	200,371	Molten corium-concrete interaction begins in calandria vault
120	431,600	Calandria vault floor failed because of concrete ablation

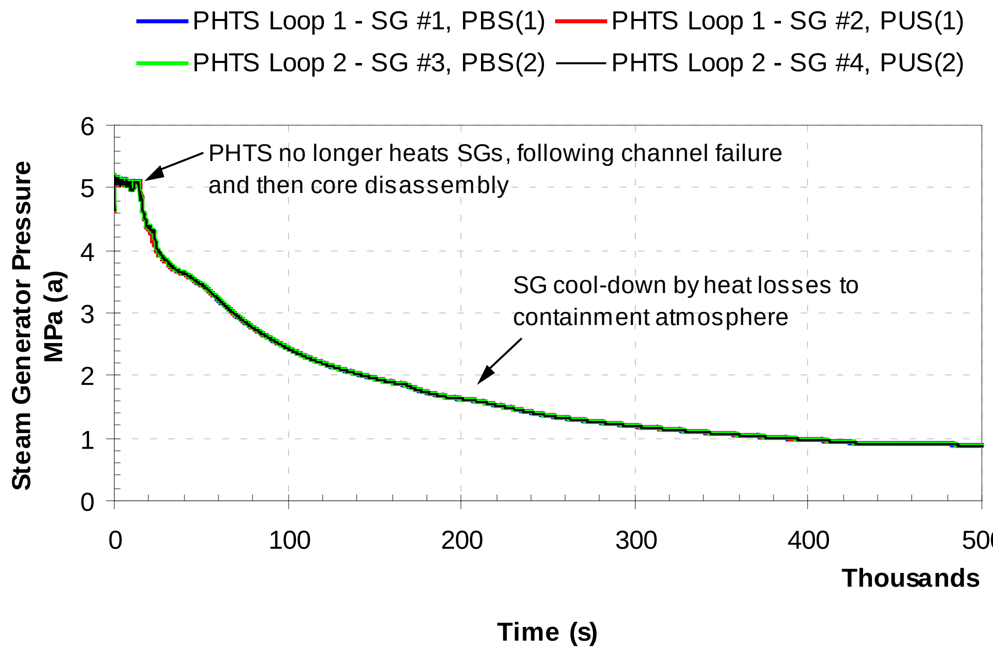

Figure 1 Steam generator secondary side pressure (0 – 500,000 s)

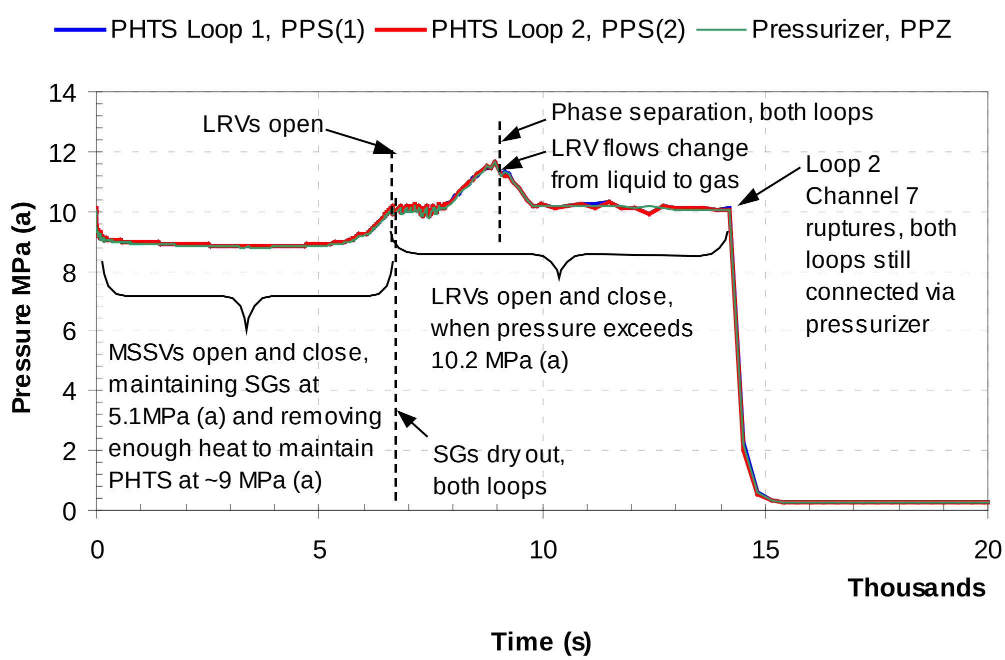

Figure 2 Pressures in PHTS and pressurizer (0 – 20,000 s)

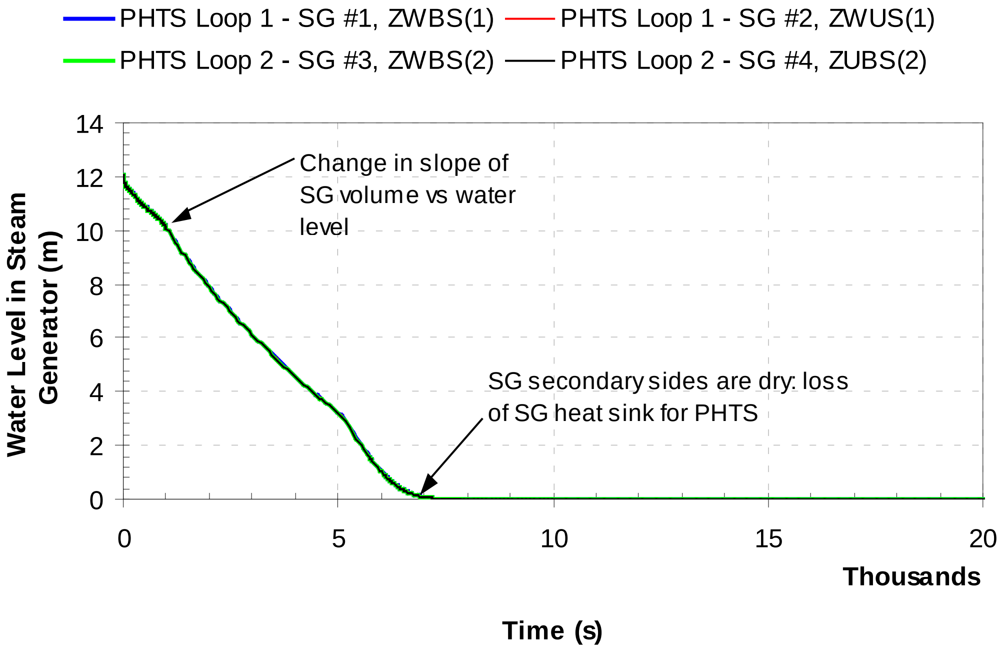

Figure 3 Steam generator water level (0 – 20,000 s)

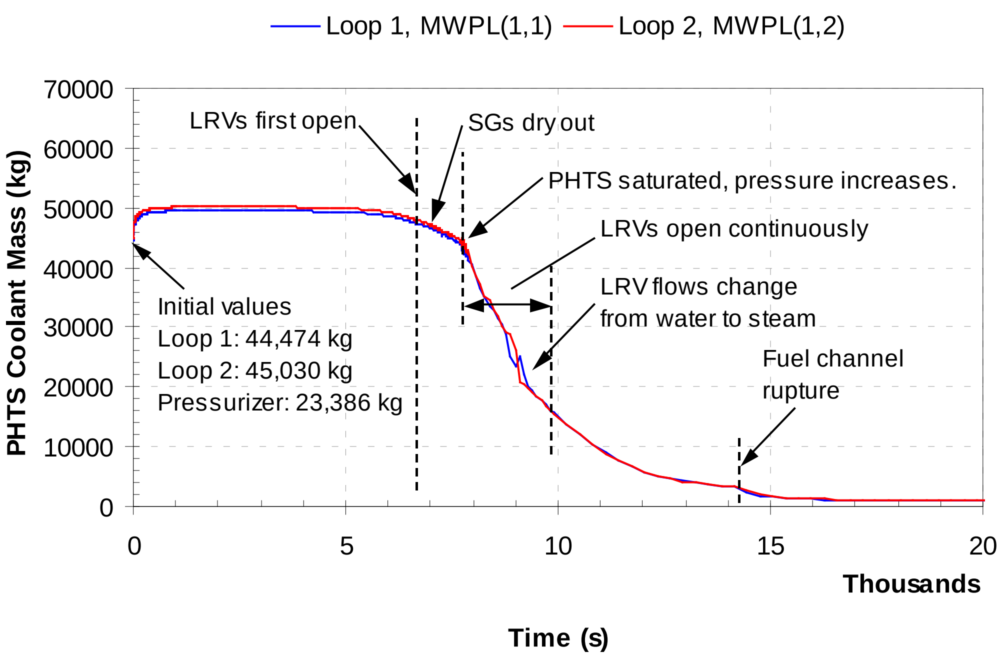

Figure 4 Water mass in PHTS loops (0 – 20,000 s)

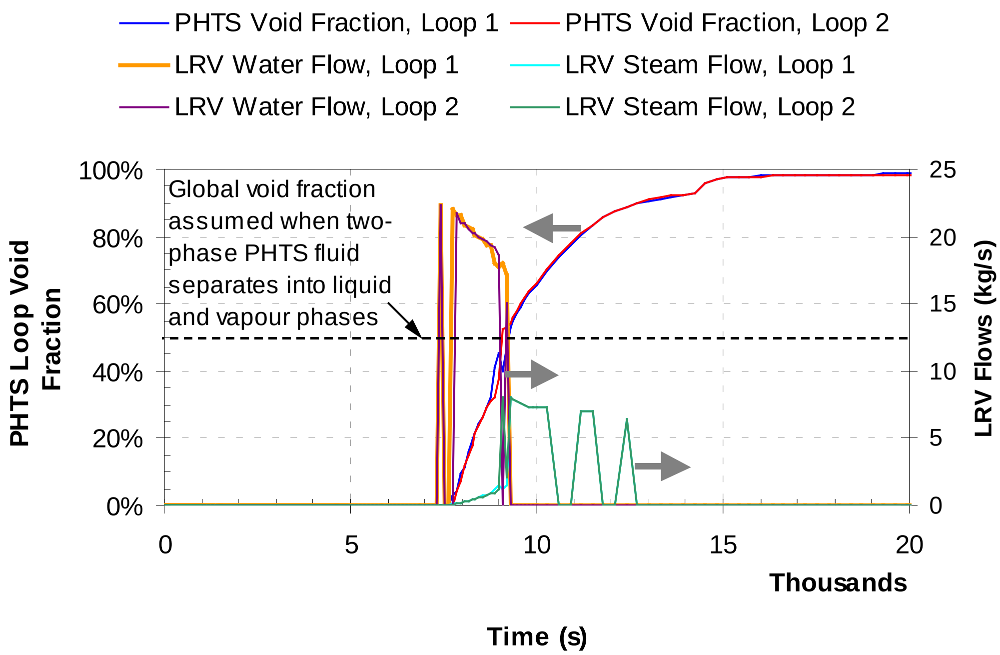

Figure 5 Loop void fractions and LRV steam / water flows (0 - 20,000 s)

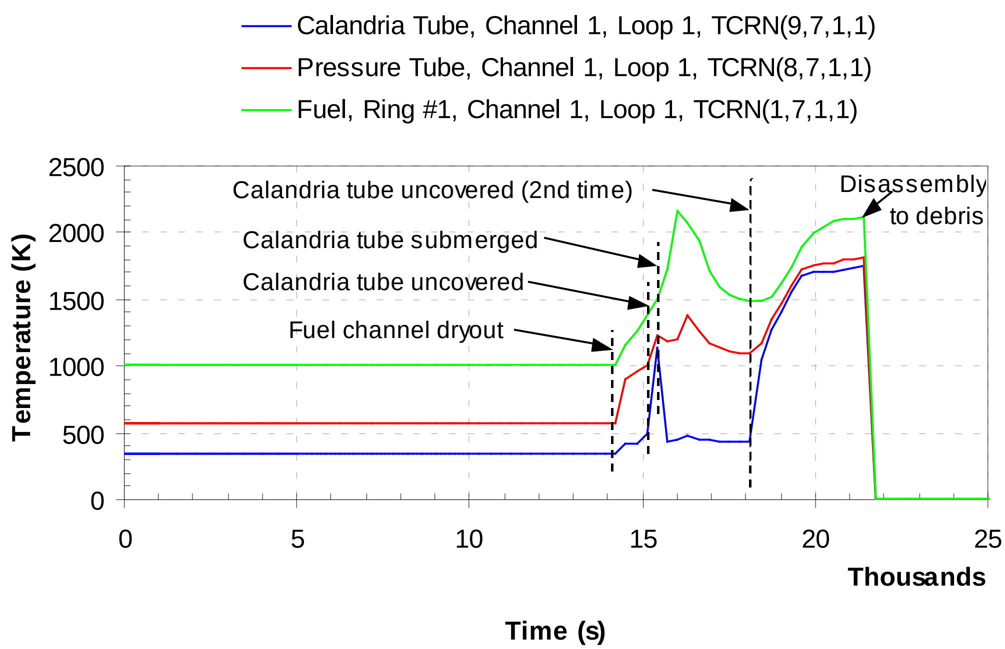

Figure 6 Fuel and fuel channel temperatures, Bundle 7, Channel 1, Loop 1 (0 - 25,000 s)

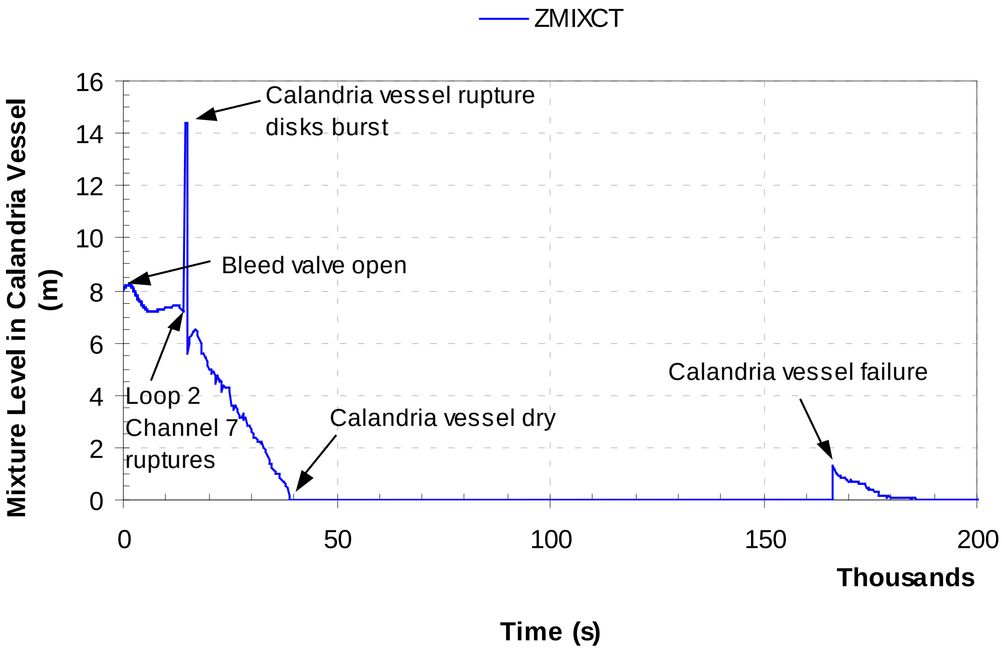

Figure 7 Calandria vessel two-phase water level (0 – 200,000 s)

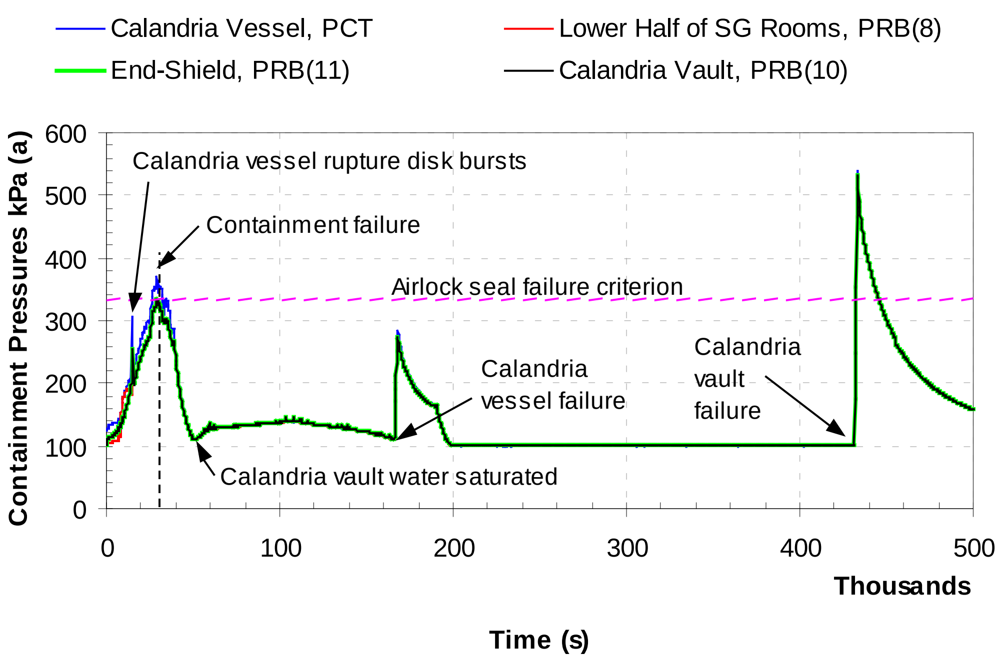

Figure 8 Containment, calandria vessel and calandria vault pressures (0 - 500,000 s)

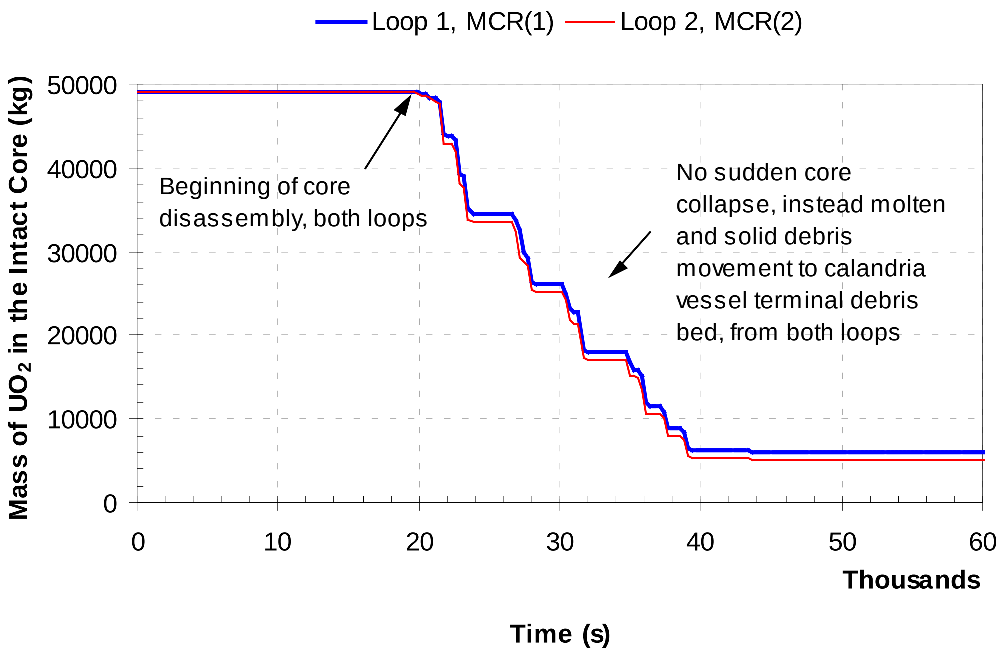

Figure 9 UO_2 mass remaining in the intact fuel channels (0 - 60,000 s)

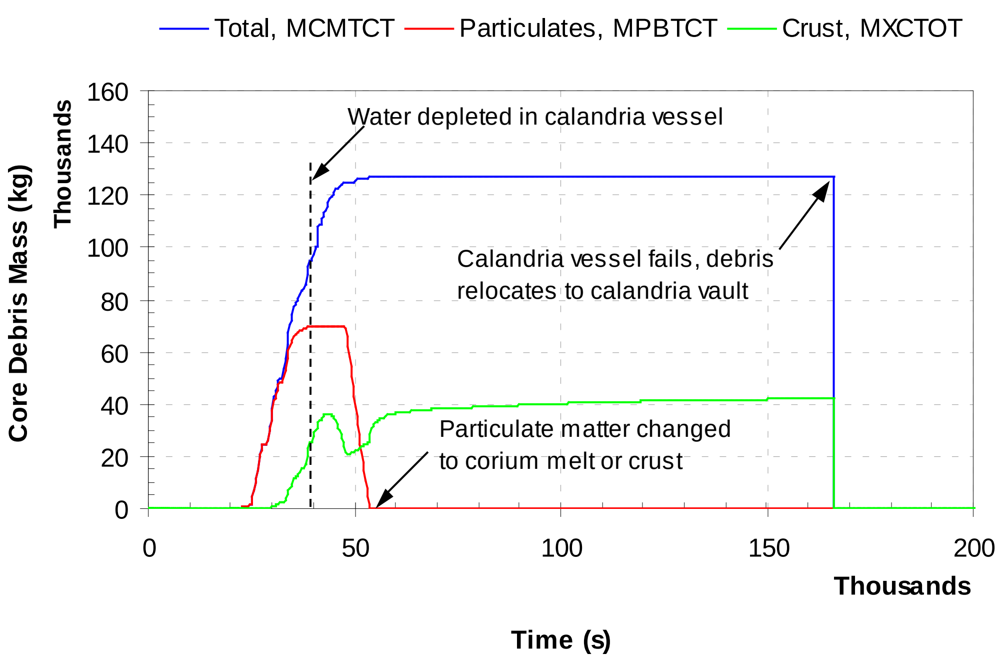

Figure 10 Mass of corium (crust, particulates and total) in the calandria vessel (0 - 200,000 s)

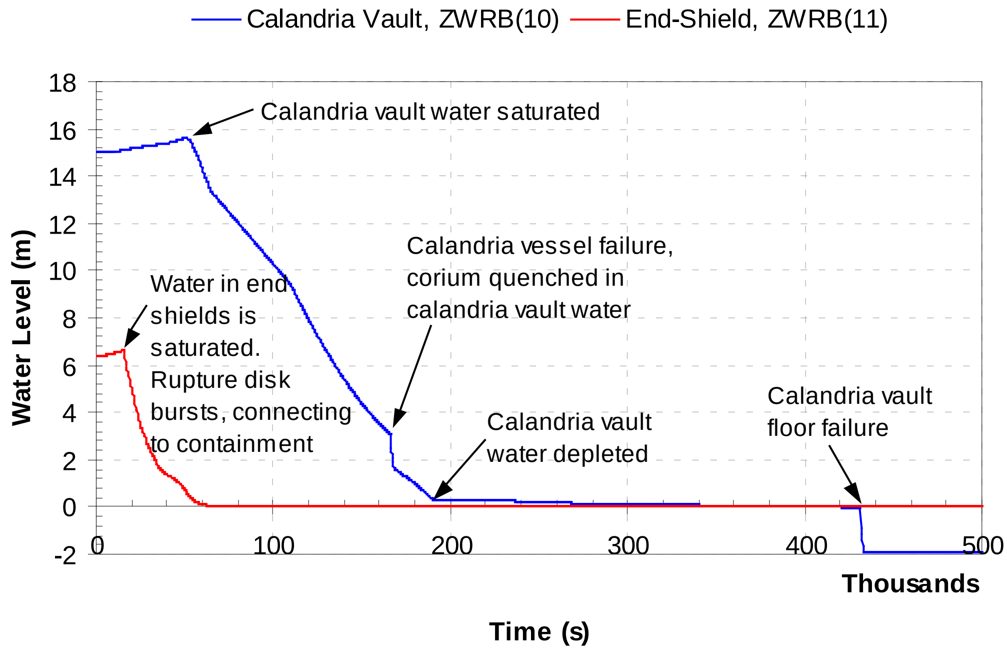

Figure 11 Calandria vault and end shield water level, Case A (0 – 500,000 s)

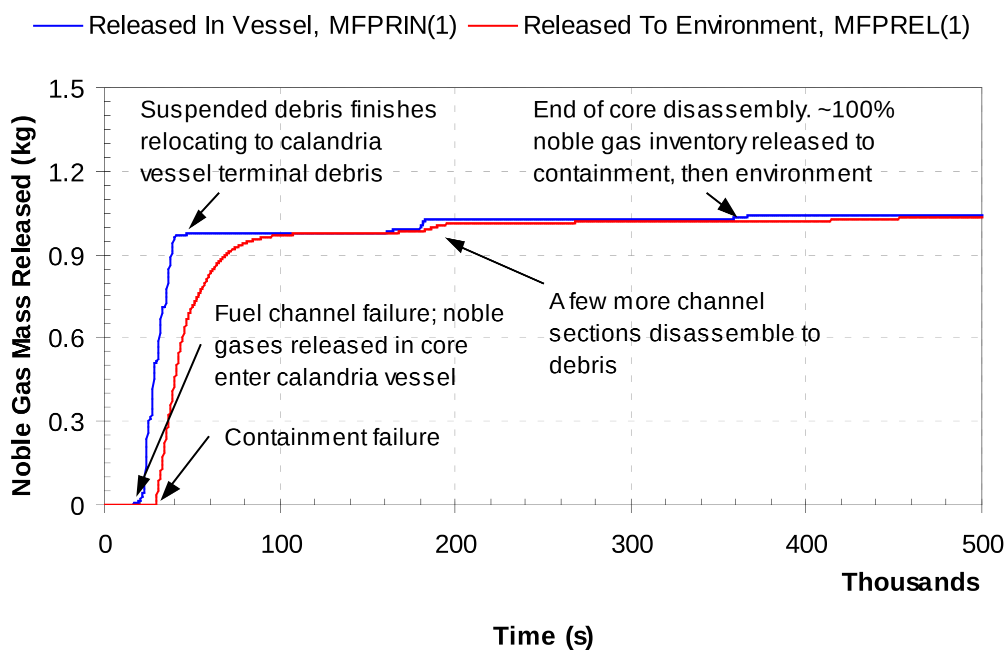

Figure 12 Mass of noble gases released (active components only) (0 - 500,000 s)

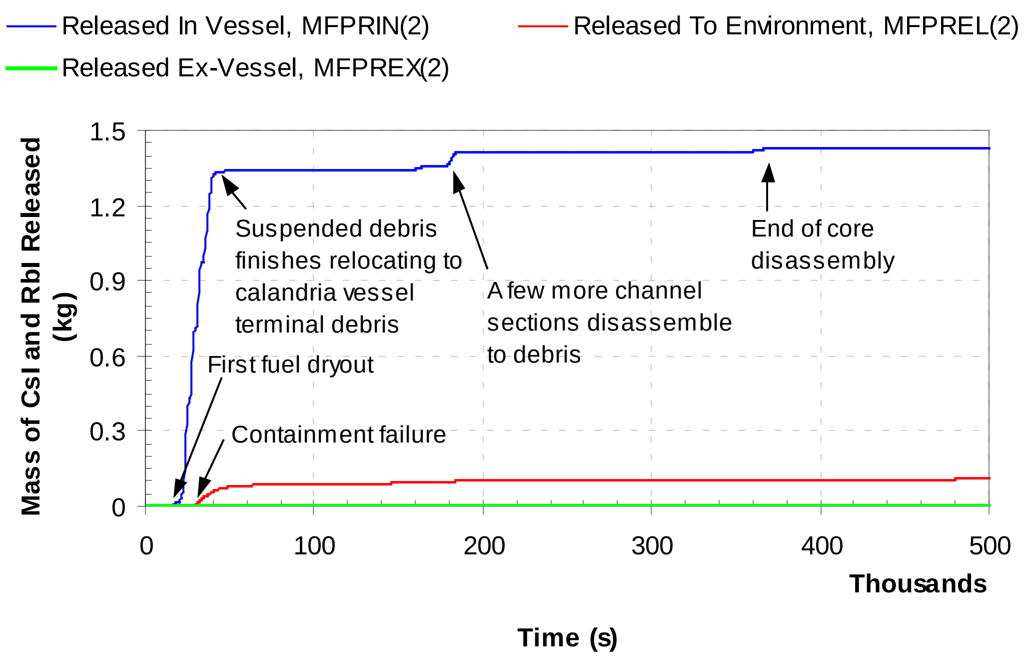

Figure 13 Mass and location of CsI releases (0 - 500,000 s)

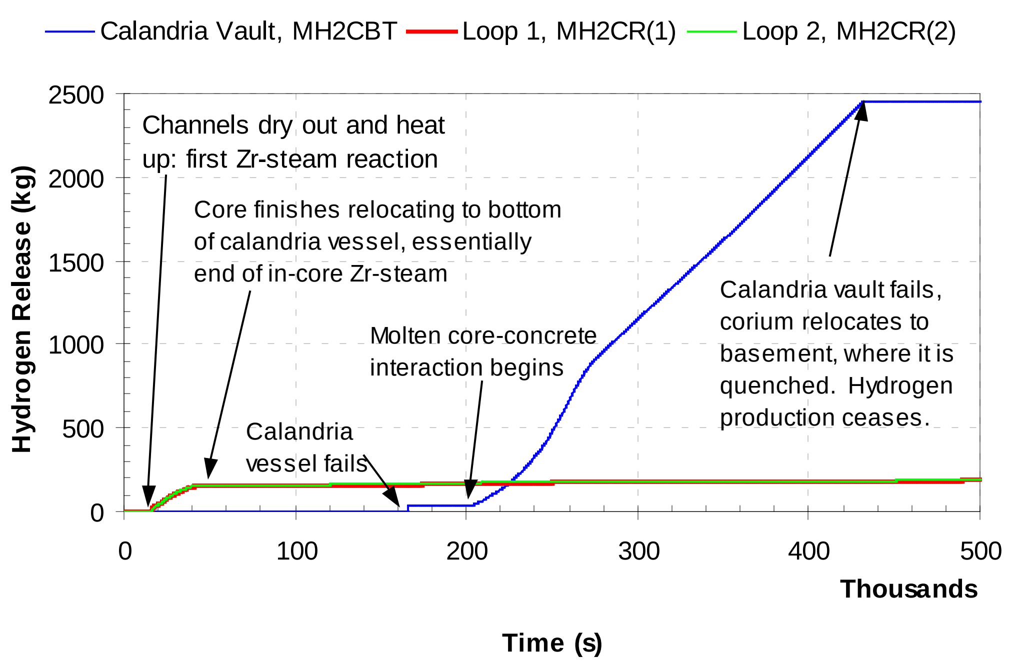

Figure 14 Hydrogen release histories in various locations (0 - 500,000 s)